Journal of Agricultural Engineering

https://www.agroengineering.org/

Co-firing performance of pellets prepared from rice husk, rice straw, and lignite in a circulating fluidized bed combustor

Volkan Çoban,[1] Kamil Ekinci,[2] Mehmet Solak,[3] Sema Yurdakul,[4] Barış Gürel,[5] Karani Kurtuluş[5]

[1]Department of Energy System Engineering, Technology Faculty, Kocaeli University, Umuttepe, İzmit/Kocaeli
[2]Department of Agricultural Machinery and Technologies Engineering, Faculty of Agriculture, Isparta University of Applied Sciences, Isparta
[3]Department of Biosystems Engineering, Faculty of Agriculture, Siirt University, Siirt
[4]Department of Environment Engineering, Süleyman Demirel University, Isparta
[5]Department of Mechanical Engineering, Süleyman Demirel University, Isparta, Türkiye

Corresponding Author: Volkan Çoban, Department of Energy System Engineering, Technology Faculty, Kocaeli University, Umuttepe, 41001 İzmit/Kocaeli, Türkiye. E-mail: volkan.coban@kocaeli.edu.tr

Publisher's Disclaimer

E-publishing ahead of print is increasingly important for the rapid dissemination of science. The *Early Access* service lets users access peer-reviewed articles well before print/regular issue publication, significantly reducing the time it takes for critical findings to reach the research community.
These articles are searchable and citable by their DOI (Digital Object Identifier).

Our Journal is, therefore, e-publishing PDF files of an early version of manuscripts that undergone a regular peer review and have been accepted for publication, but have not been through the typesetting, pagination and proofreading processes, which may lead to differences between this version and the final one.
The final version of the manuscript will then appear on a regular issue of the journal.

Please cite this article as doi: 10.4081/jae.2026.2103

©The Author(s), 2026
Licensee PAGEPress, Italy

Submitted: 16 January 2026
Accepted: 5 November 2026

***Note**: The publisher is not responsible for the content or functionality of any supporting information supplied by the authors. Any queries should be directed to the corresponding author for the article.*

All claims expressed in this article are solely those of the authors and do not necessarily represent those of their affiliated organizations, or those of the publisher, the editors and the reviewers. Any product that may be evaluated in this article or claim that may be made by its manufacturer is not guaranteed or endorsed by the publisher.

Co-firing performance of pellets prepared from rice husk, rice straw, and lignite in a circulating fluidized bed combustor

Volkan Çoban,[1] Kamil Ekinci,[2] Mehmet Solak,[3] Sema Yurdakul,[4]
Barış Gürel,[5] Karani Kurtuluş[5]

[1]Department of Energy System Engineering, Technology Faculty, Kocaeli University, Umuttepe, İzmit/Kocaeli
[2]Department of Agricultural Machinery and Technologies Engineering, Faculty of Agriculture, Isparta University of Applied Sciences, Isparta
[3]Department of Biosystems Engineering, Faculty of Agriculture, Siirt University, Siirt
[4]Department of Environment Engineering, Süleyman Demirel University, Isparta
[5]Department of Mechanical Engineering, Süleyman Demirel University, Isparta, Türkiye

Corresponding author: Volkan Çoban, Department of Energy System Engineering, Technology Faculty, Kocaeli University, Umuttepe, 41001 İzmit/Kocaeli, Türkiye. E-mail: volkan.coban@kocaeli.edu.tr

CRediT authorship contribution statement

Volkan Çoban, Conceptualization, Methodology, Project administration, Supervision, Writing – review & editing. **Kamil Ekinci,** Conceptualization, Writing – original draft. **Mehmet Solak,** Investigation, Data curation, Formal analysis. **Sema Yurdakul,** Investigation, Formal analysis, Writing – review & editing. **Barış Gürel,** Investigation, Formal analysis. **Karani Kurtuluş,** Investigation, Formal analysis.

Conflict of interests

The authors declare that they have no known competing financial interests or personal relationships that could have appeared to influence the work reported in this paper.

Data Availability Statement

The data used to support the findings of this study are available from the corresponding author on reasonable request.

Declaration of Generative AI and AI-assisted Technologies in the Writing Process

During the preparation of this work, the authors used ChatGPT (OpenAI, 2024) to improve the clarity, language consistency, and grammar of certain sections of the manuscript. After using this tool, the authors reviewed and edited the content as needed and took full responsibility for the final version of the manuscript.

Abstract

This study evaluates the co-firing performance of rice husk (RH) and rice straw (ST) pellets with and without 25% lignite addition in a 350 kW_{th} circulating fluidized bed boiler. Four pellet

formulations (RH100, RH75+CP25, ST100, and ST75+CP25) were investigated in terms of mechanical properties, thermal reactivity, and gaseous emissions. RH100 exhibited a higher vertical compressive strength than ST100 (21.55 *vs* 13.00 MPa), whereas ST100 showed higher abrasive resistance (98.02 *vs* 94.55%). The addition of 25% lignite caused modest reductions in compressive strength and abrasive resistance, while impact resistance remained high for all formulations (99.79-99.98%). Thermogravimetric analysis showed higher combustion reactivity for the pure biomass pellets than for the corresponding lignite-containing blends. Ignition temperatures increased from 221 to 245°C for the RH-based formulations and from 216 to 220°C for the ST-based formulations after lignite addition. ST100 exhibited the highest combustion indices, with Di = 0.044, S = 1.57×10^{-15}, and C = 3.68×10^{-10}. During CFBB combustion at 850±10°C, lignite addition increased CO concentrations from 1083.55 to 1803.96 mg/Nm³ for the RH-based fuels and from 1488.17 to 2832.42 mg/Nm³ for the ST-based fuels. SO_2 was not detected for the pure biomass pellets but reached 29.21 and 64.30 mg/Nm³ for RH75+CP25 and ST75+CP25, respectively, while NO emissions remained within 8.01–13.77 mg/Nm³. Overall, the results demonstrate a clear trade-off associated with 25% lignite incorporation: pellet mechanical integrity was largely retained, whereas combustion reactivity decreased and CO and SO_2 emissions increased. Among the tested formulations, the pure biomass pellets provided the most favorable overall balance of mechanical integrity, combustion reactivity, and gaseous emissions.

Key words: renewable solid fuels; co-firing; rice husk and rice straw; lignite-blended biomass; circulating fluidized bed combustion; pelletization; combustion performance and emissions.

Introduction

Rice (*Oryza sativa*) is a major component of global food systems and one of the most widely produced cereal crops. In 2021, global rice production approached 787 million metric tons, accompanied by the generation of substantial agricultural residues, namely rice husk (RH) and rice straw (ST) (FAO, 2023).

Open-field burning remains a common management practice for rice straw in several rice-producing regions. This practice releases airborne pollutants, including particulate matter, CO, and NO_x, contributing to air-quality degradation and associated environmental and health impacts (Gadde *et al.*, 2009; Singh *et al.*, 2021). Moreover, open burning results in the loss of soil nutrients and the underutilization of a potentially valuable biomass resource.

From a circular economy standpoint, RH and ST represent an abundant biomass resource with substantial potential for energy recovery (Baetge and Kaltschmitt, 2018). Among the various thermochemical conversion pathways, co-firing biomass with coal in circulating fluidized bed (CFB) combustors provides an option for the utilization of heterogeneous solid fuels. CFB systems have long been applied to the combustion and co-combustion of agricultural residues because of their flexibility toward fuels with different characteristics (Werther *et al.*, 2000). More recently, Unchaisri and Fukuda (2022) demonstrated the co-combustion of coal with 25 and 50 wt% rice straw in a 10 kW_{th} CFB reactor, providing direct experimental evidence for rice-residue co-firing under fluidized-bed conditions.

Nonetheless, RH and ST pose specific challenges due to their relatively high ash content, low bulk density, and the ash-related behavior associated with the alkali- and silica-rich mineral matter reported for rice residues. These characteristics can increase the risk of deposition, fouling, and bed agglomeration during combustion (Jenkins *et al.*, 1998; Vassilev *et al.*, 2010; Unchaisri and Fukuda, 2022). Pelletization can address several of the fuel-handling limitations associated with these residues by increasing bulk density and improving the physical consistency of the fuel. Recent studies have further shown that pelletization conditions and formulation can substantially influence the physical, mechanical, and combustion properties of rice-residue pellets (Dao *et al.*, 2022; Zhang *et al.*, 2024).

Recent research continues to highlight agricultural residues as important feedstocks for solid biomass pellet production and energy recovery (Mortadha *et al.*, 2025). Beyond pellet quality, recent studies have increasingly addressed the combustion behavior of rice-derived fuels at reactor scale. Kim *et al.* (2024) showed that air-staging conditions significantly affected NO and CO emissions during rice husk combustion in a circulating fluidized bed system, while recent CFB investigations have also demonstrated that biomass blending ratio can substantially influence combustion- and ash-related behavior during coal–rice straw co-combustion (Unchaisri and Fukuda, 2022).

Despite this progress, several research gaps remain unaddressed. Although recent studies have investigated rice-residue combustion in CFB systems, studies directly comparing lignite co-firing with RH- and ST-based pellets under identical pilot-scale conditions remain limited. Moreover, the comparative mechanical and combustion behavior of RH/ST–lignite pellet blends has rarely been evaluated by considering pellet mechanical properties, combustion reactivity, and gaseous emissions within the same experimental framework.

Importantly, previous CFB studies have generally investigated configurations in which biomass pellets and coal particles were introduced as physically separate fuel components. Such studies

provide valuable information on co-combustion behavior, but they do not address the performance of composite pellets in which the coal component is incorporated directly into the biomass matrix before combustion. The present study therefore evaluates a different fuel configuration, in which lignite powder is blended with rice husk or rice straw prior to pelletization, allowing the mechanical integrity, thermogravimetric reactivity, and pilot-scale CFBB emission behavior of the resulting biomass–lignite composite pellets to be assessed within the same experimental framework.

In response to these knowledge gaps, this study investigates four pellet formulations—100% RH, 100% ST, and their respective 75% biomass + 25% lignite blends—fired in a 350 kW_{th} circulating fluidized bed boiler. The aim is to assess not only combustion characteristics and emission profiles but also the mechanical durability and structural integrity of the pellets under realistic operating conditions.

It is hypothesized that the inclusion of 25% lignite will lead to a moderate reduction in mechanical durability due to differences in the physical properties of the fuel components, while also influencing combustion characteristics and gaseous emissions under CFB conditions. This study thus seeks to bridge the gap between laboratory characterization and pilot-scale combustion performance, offering practical insights into the viability of rice-derived agro-pellets as sustainable solid biofuels in coal–biomass co-firing scenarios.

Materials and Methods

This study employed rice husk (RH) and rice straw (ST) as primary biomass feedstocks, both derived from post-harvest rice cultivation. All samples were collected from the İpsala district of Edirne province in northwestern Turkey. The rice husks were obtained directly from local milling facilities and were utilized without additional pretreatment. In contrast, the rice straw was sourced in baled form directly from fields shortly after harvest. To minimize moisture uptake and biological degradation prior to processing, the straw was stored under controlled conditions and processed shortly thereafter. Care was taken during sample collection and handling to minimize the presence of soil and other foreign materials.

Lignite, selected as a locally available coal component, was used in the blended pellet formulations. It was pulverized prior to blending with the biomass feedstocks. All raw materials were stored under controlled conditions until preparation and experimental analysis.

Fuel preparation and pelletization

To investigate co-firing potential, four distinct pellet formulations were produced using RH, ST, and lignite coal powder (CP): RH100 (100 wt% RH), RH75+CP25 (75 wt% RH + 25 wt% CP), ST100 (100 wt% ST), and ST75+CP25 (75 wt% ST + 25 wt% CP). All feedstocks were ground and sieved to a particle size below 4 mm prior to blending and pelletization. The moisture content of the feed blends was adjusted to approximately 10–12% using a convection drying oven, with moisture content determined in accordance with ASTM D4442-20. Pelletization was conducted using a commercial flat-die pelletizer with 90 kW motor power, operating at 3.1 m/s rotor speed and a throughput of 800–1,000 kg/h. No chemical binders were added. After pelletization, the pellets were cooled at room temperature and stored in airtight containers to maintain consistent moisture content and prevent oxidative degradation prior to testing.

Representative photographs of the four pellet formulations produced in this study are presented in Figure 1, illustrating the visual appearance of the RH100, RH75+CP25, ST100, and ST75+CP25 pellets.

Physical characterization of pellets

The physical and mechanical properties of the pellets were comprehensively evaluated. Pellet diameter and length were measured using a digital caliper. Abrasive resistance was determined by placing 500 g of pellets in a rotating drum, constructed according to ASAE S269.4 DEC96 standards, and rotating it at 50 rpm for 10 min. The retained mass above a 3.15 mm sieve was measured to calculate weight loss.

Impact resistance was assessed through a modified drop test in which three randomly selected pellets from each formulation were dropped four times from a height of 1.85 meters onto a solid surface. Post-test mass was determined after sieving the samples using a 3.15 mm mesh, and the impact resistance was calculated based on retained pellet mass (Jaimes Rueda *et al.*, 2022).

Moisture sorption characteristics were examined using a controlled temperature–relative humidity conditioning approach similar to that employed in previous biomass pellet sorption studies (Bennamoun *et al.*, 2018). The pellets were first oven-dried at 105°C until constant mass was achieved and were subsequently placed in a humidity chamber at 25°C and 60% relative humidity for 9 h. Pellet masses were recorded hourly, and equilibrium moisture content was determined when the mass change stabilized (±0.01 g).

Tumbler test for pellet durability

To further assess the mechanical durability of the produced pellets against handling-related mechanical stresses, an additional tumbler-type durability test was performed. A known mass of pellets was placed into a rotating drum equipped with internal baffles and operated at 50 rpm for 10 min. Upon completion, the tumbled material was passed through a 3.15 mm sieve, and the retained mass was recorded. The durability index was calculated as the percentage of the original mass that remained intact. Mechanical durability is widely used as an important pellet-quality parameter, and recent studies have similarly evaluated pellet durability together with other physical and energetic properties (Jadwisieńczak *et al.*, 2023).

Vertical compressive strength test of pellets

To assess vertical compressive strength, a uniaxial compression test was carried out using a universal testing machine (UTM) with a 10 kN load cell. Cylindrical pellets were positioned longitudinally between two plates and compressed at 5 mm/min until structural failure. Peak load was divided by the cross-sectional area to determine compressive strength (MPa). Tests were triplicated for each type of pellet. The vertical compression test was used to quantify the resistance of the produced pellets to axial mechanical loading. Related studies have also employed controlled mechanical loading and mechanical-property measurements to characterize the behavior of densified biomass materials (Frodeson *et al.*, 2019; Stasiak *et al.*, 2020).

Proximate and ultimate analysis

Proximate analysis was performed to determine moisture, volatile matter, ash, and fixed carbon contents, using ASTM D3173, D3175, and D3174 standards. Fixed carbon was calculated by difference. Ultimate analysis was performed using a CHNS analyzer to determine the carbon, hydrogen, nitrogen, and sulfur contents, while oxygen was calculated by difference.

Higher heating value (HHV)

The HHV of each pellet blend was measured using an isoperibol bomb calorimeter per ASTM D5865/D5865M-19. HHV represents the energy potential of a fuel and is critical for evaluating combustion efficiency and system output.

Thermogravimetric analysis and determination of the combustion characteristics

Thermogravimetric analysis (TGA) was conducted to investigate the thermal decomposition behavior and combustion characteristics of the prepared pellet samples. Approximately 10 mg of each sample was analyzed using a TA Instruments Q500 thermogravimetric analyzer**,** with a heating program from ambient temperature to 800°C at a constant rate of 10°C/min under an air atmosphere (100 mL/min flow rate). The resulting thermogravimetric (TG) and derivative thermogravimetric (DTG) curves provided the basis for calculating several characteristic combustion indices.

The ignition index (Di) and comprehensive combustion index (S) were calculated based on thermogravimetric combustion parameters following the approach described by Wnorowska *et al.* (2021). The flammability index (C) was calculated separately as described below.

In addition to individual interpretation, a set of combustion indices was employed for cross-sample comparison. These parameters enabled a comparative evaluation of ignition behavior and combustion reactivity across the different pellet formulations under identical thermogravimetric conditions.

To evaluate overall combustion performance, the Comprehensive Combustion Index (S) was calculated using Eq. (1). A higher S value indicates greater fuel reactivity and combustion intensity, thereby facilitating comparison of combustion behaviors between samples (Liu *et al.*, 2025)**:**

$$S = \frac{(\frac{d_W}{d_t})_{max}(\frac{d_W}{d_t})_{avg}}{T_i^2\, T_b} \qquad \text{(Eq. 1)}$$

This equation incorporates several key parameters: the maximum weight loss rate (expressed in %/min) represents the peak rate of thermal decomposition during combustion, while the average weight loss rate provides an overall measure of mass reduction across the combustion range. The ignition temperature (Ti) denotes the point at which rapid volatilization begins, marking the onset of significant mass loss, and the burnout temperature (Tb) indicates the stage where combustion reactions approach completion and the remaining carbonaceous residue is oxidized. Together, these variables form a robust basis for assessing the fuel's overall combustion reactivity and efficiency.

The ignition temperature (Ti) was determined from the TG curve using the intersection-of-tangents method. A first tangent was drawn approximately parallel to the baseline before the onset of rapid mass loss, while a second tangent was drawn at the point corresponding to the maximum mass-loss rate. The intersection of these tangents was taken as Ti. The burnout temperature (Tb) was defined as the temperature at which 98% of the total combustible mass

loss had been completed. The peak temperature (Tp) was identified directly from the DTG curve as the temperature corresponding to the maximum mass-loss rate. These characteristic temperatures were determined following the approach described by Wnorowska *et al.* (2021).

The Ignition Index (Di), which quantifies the ease of ignition, was computed using Eq. (2) following the approach of Wnorowska *et al.* (2021):

$$D_i = \frac{DTGmax}{t_i\, t_p} \qquad \text{(Eq. 2)}$$

In this formulation, DTG_{max} refers to the maximum rate of weight loss (%/min) observed during thermal decomposition, which signifies the most intense stage of combustion. The ignition time (ti) represents the duration from the start of heating until the onset of rapid mass loss, indicating when volatile release initiates. The time at maximum weight loss rate (tp) corresponds to the moment when DTG_{max} occurs, reflecting the peak of devolatilization and combustion activity. These parameters collectively offer insight into the fuel's ignition responsiveness and combustion kinetics.

The Flammability Index (C), which serves as an indicator of initial combustion reactivity under thermogravimetric conditions, was calculated using Eq. (3):

$$C = \frac{(\frac{d_w}{d_t})max}{T_i^2} \qquad \text{(Eq. 3)}$$

Higher C values are generally associated with greater initial combustion reactivity under thermogravimetric conditions (Qin *et al.*, 2022). Together, the calculated indices provide a quantitative basis for comparing the ignition characteristics and combustion reactivity of the pellet formulations under identical experimental conditions.

Combustion testing in circulating fluidized bed boiler

Combustion trials were conducted in a 350 kW_{th} pilot-scale CFBB. Each pellet formulation was tested individually at 850 ± 10°C, with a fluidization velocity of 1.2–1.4 m/s. Silica sand (250–500 μm) was used as bed material. Air-to-fuel ratios were optimized for stable fluidization. Emissions were continuously monitored using a CEMS calibrated to EN 14181 standards.

Characteristic combustion parameters and emissions

Key combustion parameters were derived from the TG and DTG curves to characterize the combustion behavior of the pellet samples. The characteristic combustion parameters included the ignition temperature (T_i), peak temperature (T_p), burnout temperature (T_b), maximum mass-loss rate (DTG_{max}), and total combustion duration. T_i, T_p, and T_b were determined as previously

described. These parameters were used as comparative indicators of fuel reactivity and thermochemical behavior under oxidative conditions.

In parallel, flue gas emissions were continuously monitored during combustion using a calibrated Continuous Emission Monitoring System (CEMS). Quantification of the major gaseous species was carried out with advanced detection methods: carbon dioxide (CO_2) concentrations were measured via non-dispersive infrared (NDIR) spectroscopy; sulfur dioxide (SO_2) levels were assessed using ultraviolet fluorescence; carbon monoxide (CO) concentrations were determined electrochemically; and nitric oxide (NO) levels were analyzed through chemiluminescence. Emission measurements were performed after stable combustion conditions were established. For each fuel formulation, emissions were recorded at 1-s intervals during three 30-min measurement periods. Data corresponding to clearly identifiable abnormal operating conditions were excluded, whereas routine fuel-feeding periods were retained as part of normal boiler operation. The valid second-by-second data from the three measurement periods were pooled, and the arithmetic mean and standard deviation were calculated for each emission parameter. All emission values were standardized to reference conditions of 0°C, 1 atm pressure, and 6% O_2 in accordance with the Directive 2010/75/EU on industrial emissions.

Experimental setup

Pelletization system description

The densification of the fuel mixtures was performed using a commercial-scale flat-die pelletizer designed for continuous biomass processing. The system operated with a 90 kW motor and maintained a throughput capacity ranging from 800 to 1,000 kg/h, depending on feedstock properties and moisture content.

Prior to pelletization, the raw materials, including rice husk, rice straw, and lignite were subjected to a mechanical pre-processing stage that included shredding and blending. A horizontal mixer was integrated into the system to ensure homogeneity in particle size (below 4 mm) and uniform moisture distribution across each blend. These steps were critical to producing pellets with consistent structure and mechanical integrity.

Pelletization was carried out at a rotor surface velocity of 3.1 m/s. This speed was selected to balance die pressure and energy input, avoiding issues such as thermal degradation or structural cracking of the feedstock. The flat-die configuration allowed stable operation under a range of feeding conditions and eliminated the need for chemical binders. A photograph of the commercial-scale flat-die pelletization system used in this study is presented in Figure 2.

Once extruded, pellets were air-cooled to ambient temperature under controlled conditions and then stored in moisture-proof containers to prevent rehydration or oxidation prior to further

testing. This setup provided consistent, scalable pellet production suitable for combustion testing in fluidized bed systems.

Circulating fluidized bed boiler (CFBB)

Combustion tests were performed using a pilot-scale circulating fluidized bed boiler (CFBB) with a nominal thermal capacity of 350 kW_{th}, specifically designed for biomass and lignite co-firing research. The system incorporated a monolithic cast refractory combustion chamber, providing enhanced structural integrity and thermal insulation under high-temperature operation. The pilot-scale CFBB experimental system used in the combustion tests is shown in Figure 3.

The fuel feeding system utilized dual screw feeders to independently supply lignite (up to 400 kg/h) and biomass (up to 100 kg/h) at a feed height of 0.8 m from the base of the chamber. Quartz sand, with a particle size range of 200–700 μm and a bulk density of 1,650 kg/m³, was employed as the bed material. A total of 60 kg of sand was loaded to achieve a static bed height of 0.3 m.

Primary fluidization was achieved by a 15 kW centrifugal blower delivering a maximum airflow rate of 1,000 m³/h at 300 mbar pressure, while seal-pot fluidization air was maintained at a rate of 0.01 kg/s.

System start-up involved preheating via a 300 kW diesel burner, consuming approximately 30 L/h of fuel. Positioned 1.8 m above the chamber base and supported by an LPG–O_2 ignition flame, the burner operated until the bed temperature reached 800°C, at which point the system transitioned to self-sustaining combustion.

Real-time thermal monitoring was conducted using K-type thermocouples (±1°C accuracy), encased in ceramic and steel, and strategically positioned at vertical heights of 30, 530, 980, and 1,740 mm within the combustion chamber. The chamber geometry was rectangular, measuring 0.54 m × 0.23 m up to a height of 1.0 m, then expanding to 0.54 m × 0.30 m. The overall combustion zone length was 2 m, followed by a 1.5 m heat recovery section with integrated water-cooled heat exchange pipes. The total system extended to a length of 5.46 m.

For steam generation and thermal energy recovery, a closed-loop water circulation system was employed. A 1 kW submerged pump delivered up to 400 L/h of water at 1 bar pressure to a steam drum located 5.6 m above ground level. The circulation circuit included a 500 L feed tank and a 300 L steam drum, offering a cumulative heat exchange surface area of 3.6 m².

This integrated CFBB setup offers a realistic and controllable environment for investigating co-firing dynamics, providing reliable data on combustion efficiency, emission performance, and operational stability under near-industrial conditions.

Results and Discussion

Chemical properties

The proximate and ultimate analysis results of RH, ST, and lignite are summarized in Table 1. According to the elemental analysis results, both RH and ST exhibit similar characteristics in terms of carbon (41.8% and 41.5%), hydrogen (5.7% and 5.5%), and oxygen content (49.8% and 50.7%). These findings are consistent with previous studies indicating that rice-based biomass typically presents a moderate carbon concentration along with a high volatile matter content (Jenkins *et al.*, 1998). For instance, Mansaray and Ghaly (1997) reported variation in the elemental composition among six rice husk varieties, while Lim *et al.* (2012) reported values of 38.83% C, 4.75% H, and 0.52% N for rice husk. Compared with the values reported by Lim *et al.* (2012), the RH sample examined in the present study exhibited somewhat higher carbon (41.8 vs. 38.83%) and hydrogen (5.7 vs. 4.75%) contents, whereas a more pronounced difference was observed for nitrogen (2.70 vs. 0.52%).

The oxygen content in both biomasses exceeded 49%, indicating the highly oxygenated nature of the rice residues investigated. Baetge and Kaltschmitt (2018) emphasized that such high oxygen levels are common in biomass and are generally associated with lower energy density. The higher heating values (HHV) measured in the present study were 14.84 MJ/kg for RH and 14.75 MJ/kg for ST. These values are consistent with those reported for rice-derived residues in the literature. Lim *et al.* (2012) reported HHVs of 15.84 MJ/kg for rice husk and 15.09 MJ/kg for rice straw, while Kaniapan *et al.* (2022) summarized literature ranges of 14.61–15.44 MJ/kg and 12.10–16.60 MJ/kg for rice husk and rice straw, respectively. The present results therefore fall within, or close to, the range of values previously reported for these residues.

Sulfur content was negligible in both biomass samples, which contributes to their low SO_2 formation potential and provides an environmental advantage over sulfur-containing fossil fuels. In contrast, the lignite contained 4.42% sulfur, indicating that lignite addition can increase the sulfur input of the blended fuels. This is consistent with the SO_2 emissions observed during the subsequent CFBB combustion tests. The negligible sulfur content of RH and ST agrees with prior research identifying rice-based biomass as inherently low in sulfur (Vassilev *et al.*, 2010; Mortadha *et al.*, 2025). The nitrogen contents of RH and ST were 2.70% and 2.30%, respectively, while lignite contained 1.87% nitrogen. These values indicate that fuel-bound

nitrogen may contribute to NO formation during combustion and should therefore be considered when interpreting the emission results.

In terms of proximate composition, both RH and ST exhibited volatile matter contents of approximately 65% which were lower than the values commonly reported for wood pellets, typically around 76-82% (Stolarski *et al.*, 2022). Ash contents were 16.00% for RH and 15.50% for ST, substantially higher than the ash limits specified for ENplus® wood-pellet classes (A1: ≤0.70%, A2: ≤1.20%, and B: ≤2.00%). The relatively high ash contents indicate that these fuels require combustion systems with appropriate ash-handling capability; ISO 17225-6:2021 similarly notes that non-woody pellets should preferably be used in appliances specifically designed or adjusted for such fuels. The HHVs measured for RH and ST (14.84 and 14.75 MJ/kg, respectively) were lower than values commonly reported for wood pellets, which are approximately 19-21 MJ/kg, but remained consistent with previously reported values for rice-derived residues.

The mineral composition of the ash, including the SiO_2 content, was not experimentally quantified in the present study. Therefore, no sample-specific silica content is reported for RH or ST. Nevertheless, previous studies have consistently identified silica as a major inorganic constituent of rice husk and rice straw ash (Jenkins *et al.*, 1998; Vassilev *et al.*, 2010; Beidaghy Dizaji *et al.*, 2019). Detailed ash characterization, including SiO_2 quantification, should therefore be considered in future studies.

The importance of this limitation is supported by Unchaisri and Fukuda (2022), who investigated rice-straw pellets co-fired with granular coal in a CFB reactor and reported substantially greater fouling deposition during biomass–coal co-combustion than during pure-coal combustion. At a biomass fraction of 50 wt%, the rice-straw/coal blend produced the highest deposit among the biomass fuels investigated, and deposit formation increased with increasing biomass fraction. The authors related this behavior to the ash characteristics of rice straw, including the contribution of K-, Ca-, and Si-containing species. Although these findings cannot be transferred quantitatively to the present composite pellets, they indicate that ash deposition and fouling should be specifically evaluated in future long-duration CFBB tests of ST–lignite pellets.

Differences in elemental composition relative to literature values may reflect variability among rice varieties, cultivation regions, and growing conditions, as reported for both rice straw and rice husk in recent literature. Overall, these findings support the potential use of rice residues from the Edirne region as solid biofuels in appropriately designed combustion systems.

Mechanical properties of the pellets

The mechanical properties of biomass pellets are critical indicators of their suitability for transportation, storage, and combustion performance. In this study, four different pellet formulations—RH100, RH75+CP25, ST100, and ST75+CP25—were systematically assessed based on six key indicators: particle diameter, length, weight, abrasive resistance, impact resistance, and vertical compressive strength, as summarized in Table 2.

The average diameters across all samples remained relatively uniform, ranging from 8.16 mm to 8.50 mm. However, pellet length varied significantly, with ST100 pellets reaching an average of 39.67 mm substantially longer than RH75+CP25 at 29.1 mm. The inclusion of 25% lignite was accompanied by reductions in the average pellet length and weight for both RH- and ST-based formulations.

Abrasive resistance, reflecting a pellet's durability under tumbling and mechanical friction, was highest in ST100 at 98.02%, followed by RH100 at 94.55%. With 25% lignite addition, abrasive resistance decreased to 89.10% for RH75+CP25 and 93.22% for ST75+CP25. These results indicate that lignite incorporation was associated with reduced resistance to mechanical degradation in both biomass-based pellet formulations. Interestingly, Gil *et al.* (2010) reported that low coal additions (up to 20% in selected biomass–coal blends) did not reduce pellet durability, indicating that the mechanical response to coal incorporation can depend on feedstock type and blend composition.

All pellet types exhibited excellent impact resistance, with values ranging from 99.79% to 99.98%, indicating that neither biomass type nor 25% lignite incorporation substantially affected resistance to impact-induced breakage.

Vertical compressive strength was highest for RH100 at 21.55 MPa. In contrast, ST100 exhibited a lower compressive strength of 13.00 MPa. The addition of 25% lignite was accompanied by modest reductions in compressive strength, from 21.55 to 20.62 MPa for the RH-based pellets and from 13.00 to 12.24 MPa for the ST-based pellets. Previous studies indicate that the mechanical response of biomass–lignite densified fuels can vary with feedstock composition and formulation. For example, Özyuğuran *et al.* (2017) reported improved mechanical strength when rice husk was added to lignite-based briquettes, whereas the present study showed a modest reduction when lignite was incorporated into biomass-based pellets.

The lower compressive strength observed for ST-based pellets may be related, at least in part, to compositional differences between rice straw and rice husk. Zulkornain *et al.* (2022) reported lower natural lignin content in rice straw than in rice husk and found that rice straw pellets required greater binder and moisture addition to achieve high durability. Lignin acts as a natural

thermoplastic binder during pelletization and can contribute to interparticle bonding and pellet strength under suitable temperature and moisture conditions (Tumuluru, 2018). Similarly, Do *et al.* (2025) identified low lignin content as a technical challenge in rice straw pelletization and demonstrated that pellet durability is influenced by pelletizing conditions and binder addition. In the present study, incorporating 25% lignite into ST pellets reduced compressive strength from 13.00 to 12.24 MPa, whereas impact resistance remained essentially unchanged (99.79–99.98%). These findings indicate that the mechanical effect of lignite incorporation was dependent on the measured property rather than representing a uniform deterioration of pellet integrity.

These mechanical trends are summarized in Figure 4 a,b, highlighting the higher compressive strength of RH-based pellets, the higher abrasive resistance of ST-based pellets, and the modest reductions in both properties following 25% lignite incorporation.

Overall, the comparative evaluation indicates that RH-based pellets exhibited higher compressive strength than ST-based pellets, whereas ST-based pellets showed higher abrasive resistance. These findings validate the potential for RH- and ST-based hybrid pellets in industrial applications where mechanical stability during transport, storage, and automated feeding is critical.

Combustion characteristics

The combustion behavior of the four pellet formulations (RH100, RH75+CP25, ST100, and ST75+CP25) was analyzed through thermogravimetric techniques, and the key combustion parameters derived from DTG curves are summarized in Table 3. These include ignition temperature, burnout temperature, peak decomposition rate, and combustion indices, providing a quantitative basis for comparing the thermal reactivity and combustion characteristics of each blend under identical thermogravimetric conditions.

Thermogravimetric analysis (TGA) revealed marked distinctions in combustion behavior among the tested pellet formulations. Among the four blends, ST100 and ST75+CP25 exhibited the lowest ignition temperatures -216°C and 220°C, respectively- indicating greater initial reactivity compared to rice husk-based formulations. Conversely, RH75+CP25 displayed the highest ignition temperature (245°C), indicating delayed ignition after lignite incorporation.

For RH100, the highest-temperature DTG peak occurred at 453.2°C, while the TGA-derived burnout temperature (Tb) was 520.2°C. These temperatures, together with the combustion indices, were used to compare the thermal behavior of the formulations.

Combustion indices derived from DTG data provided further quantitative insight into the thermal reactivity and combustion behavior of each blend under the applied thermogravimetric conditions. The ignition index (Di) was highest for ST100 (0.044), followed by ST75+CP25 (0.040), confirming that straw-based pellets ignite more readily. This is attributable to their higher volatile content and fibrous morphology, which facilitate more rapid oxidation.

Among the samples studied, ST100 recorded the highest Comprehensive Combustion Index (S) at 1.57×10^{-15}, followed by RH100 at 1.39×10^{-15}. These findings indicate that pure biomass formulations exhibit better overall combustion reactivity than their corresponding lignite-containing blends. Regarding the flammability index (C) which reflects chemical reactivity during the initial stage of combustion, ST100 again showed the highest value (3.68×10^{-10}). The C values decreased from 3.16×10^{-10} to 2.37×10^{-10} for the RH-based formulations and from 3.68×10^{-10} to 3.31×10^{-10} for the ST-based formulations after 25% lignite addition, indicating lower initial combustion reactivity under the applied thermogravimetric conditions. These trends are directionally consistent with Qin *et al.* (2022), who reported substantially greater ignition and combustion indices for rice straw than for bituminous coal, and with Aich and Nandi (2025), who observed progressively enhanced combustion reactivity as the rice-straw fraction increased in rice straw–coal blends. The incorporation of lignite generally shifted the combustion behavior toward lower reactivity, which can be related to the marked difference in volatile matter between biomass and lignite. While RH and ST contained approximately 65% volatile matter, the corresponding value for lignite was 31.4%. The higher volatile content of the biomass promotes rapid devolatilization and facilitates ignition, whereas lignite addition reduces the volatile fraction of the blend and increases the relative contribution of the slower char-oxidation stage. This effect was particularly evident for RH75+CP25, for which the ignition and burnout temperatures increased from 221 to 245°C and from 520.2 to 538.1°C, respectively.

This interpretation is also consistent with previous rice straw–coal co-combustion studies reporting enhanced ignition and overall combustion reactivity with increasing biomass fraction (Qin *et al.*, 2022; Aich and Nandi, 2025). The corresponding ignition-to-burnout temperature ranges and the relative retention of the combustion indices after lignite addition are illustrated in Figure 4 c,d. Compared with the corresponding pure biomass pellets, RH75+CP25 retained approximately 86.1%, 70.8%, and 75.0% of the Di, S, and C values, respectively, whereas ST75+CP25 retained 90.9%, 85.4%, and 89.9%. The incorporation of lignite generally reduced ignition and overall combustion reactivity, while its effect on the TGA-derived burnout

temperature depended on the biomass type. A more pronounced increase in burnout temperature was observed for the RH-based formulation than for the ST-based formulation.

Flue gas emissions

The flue gas emission profiles obtained from CFBB tests for the four pellet formulations are summarized in Table 4, allowing a descriptive comparison of the measured concentrations of carbon monoxide (CO), sulfur dioxide (SO_2), nitric oxide (NO), and carbon dioxide (CO_2).

The lignite-containing blends exhibited higher mean CO concentrations than the corresponding pure biomass formulations. ST75+CP25 showed the highest mean CO concentration at 2832.42 mg/Nm³, followed by RH75+CP25 at 1803.96 mg/Nm³, whereas RH100 and ST100 exhibited lower values of 1083.55 and 1488.17 mg/Nm³, respectively. The higher mean CO concentrations observed for the lignite-containing blends may be associated with their lower combustion reactivity and the substantially lower volatile matter content of lignite (31.4%) compared with RH and ST (65.37% and 65.73%, respectively). Incomplete CO oxidation may also have been affected by short-term variations in local oxygen availability and air-to-fuel ratio during fuel feeding. Unchaisri *et al.* (2019) similarly demonstrated that CO emissions during biomass–coal co-firing in a CFB are highly sensitive to excess air, bed temperature, and residence time, emphasizing the importance of combustion conditions in addition to fuel-blend composition.

The relatively large standard deviations observed for CO can be interpreted as reflecting temporal fluctuations during normal CFBB operation. Emissions were recorded at 1-s intervals during three 30-min measurement periods, and routine fuel-feeding periods were retained as part of normal boiler operation, whereas clearly identifiable abnormal operating periods were excluded. Since the pilot-scale CFBB employed manual rather than PLC-based automatic air-to-fuel ratio control, the observed CO variability may be attributed to short-term variations in oxygen availability and the air-to-fuel ratio during fuel feeding. CO, being particularly sensitive to incomplete combustion and local oxygen deficiency, consequently exhibited greater temporal variability than the other measured gaseous emissions.

Furthermore, when compared to commonly used biomass types such as woodchips and wheat straw, which typically emit CO in the range of 400–1000 mg/Nm³ under optimized combustion conditions, the values recorded in this study, although moderate, point to room for optimization (Werther *et al.*, 2000, Saidur *et al.*, 2011). Since CO formation is strongly influenced by local oxygen availability, mixing conditions, and the air-to-fuel ratio, improved fuel-feeding control and automated combustion-air regulation could reduce both CO concentrations and their

temporal fluctuations. Accordingly, the CO concentrations reported here should be regarded as representative of the tested combustion conditions rather than as intrinsic emission factors of the pellet formulations. In practical applications, CO emissions should therefore be regarded as a combustion-performance parameter that can be controlled through appropriate fuel-feeding and air-supply regulation.

Given the large temporal variability in CO concentrations, particularly for ST75+CP25, the observed differences among the mean values should be interpreted descriptively rather than as statistically significant differences between fuel formulations.

Nitric oxide (NO) emissions remained within a relatively narrow range of 8.01–13.77 mg/Nm³, with the highest mean concentration observed for RH75+CP25. However, this increase cannot be directly attributed to the nitrogen content of lignite, since lignite contained less nitrogen (1.87%) than both RH (2.70%) and ST (2.30%). At the relatively low CFBB operating temperature used in this study (850 ± 10°C), NO formation is expected to be governed predominantly by fuel-nitrogen conversion and local combustion conditions rather than by the thermal-NO pathway. Previous CFB studies have likewise shown that NO emissions are sensitive to fuel composition and combustion conditions such as excess air and air staging (Unchaisri *et al.*, 2019; Kim *et al.*, 2024).

Sulfur dioxide (SO_2) was not detected during combustion of the pure biomass formulations, consistent with the negligible sulfur content measured for RH and ST. In contrast, measurable SO_2 concentrations were observed for the lignite-containing blends, reaching 29.21 mg/Nm³ for RH75+CP25 and 64.30 mg/Nm³ for ST75+CP25. This increase is consistent with the substantially higher sulfur content of lignite (4.42%) compared with the negligible sulfur content of the two biomass fuels. Thus, under the tested CFBB conditions, lignite incorporation clearly increased sulfur input and the corresponding SO_2 emissions.

The present results can also be considered in the context of the closely related CFB study of Unchaisri and Fukuda (2017). In that study, separately produced rice-straw pellets were co-fed with coal at biomass mass fractions of 25 and 50%, and increasing the rice-straw fraction resulted in lower NO_x and SO_2 emissions but higher CO concentrations. In contrast, the present ST75+CP25 formulation contained 75% rice straw and 25% lignite incorporated within the same pellet. Relative to ST100, lignite incorporation increased CO from 1488.17 to 2832.42 mg/Nm³ and resulted in measurable SO_2 emissions of 64.30 mg/Nm³. The opposite SO_2 trends are consistent with the different blending directions: increasing the biomass fraction diluted the sulfur-containing coal contribution in the former study, whereas lignite addition increased the sulfur input in the present study. The CO response in both studies nevertheless emphasizes the

sensitivity of CFB co-combustion to fuel composition and combustion-air conditions. Direct quantitative comparison should be made cautiously because the studies differed in biomass-to-coal ratio, coal type, fuel configuration, reactor scale, and operating conditions.

The principal distinction of the present study therefore lies in the fuel architecture rather than in co-firing alone. In the study of Unchaisri and Fukuda (2017), rice-straw pellets and coal remained physically discrete fuel particles during feeding and combustion, whereas in the present work lignite powder was incorporated directly into the rice-straw matrix before pelletization to form the ST75+CP25 composite fuel. The resulting composite pellet retained substantial mechanical integrity: compared with ST100, vertical compressive strength decreased from 13.00 to 12.24 MPa and abrasive resistance from 98.02 to 93.22%, while impact resistance remained essentially unchanged. At the same time, lignite incorporation was accompanied by an increase in ignition temperature from 216 to 220 °C, decreases in the Di, S, and C indices, and increases in CO and SO_2 emissions relative to ST100. These results show that incorporating lignite directly into the rice-straw pellet produces a mechanically viable composite fuel, but with measurable changes in thermal reactivity and gaseous-emission behavior.

Because the present experiments did not include a separately co-fed ST–lignite mixture of identical 75/25 composition, these changes cannot be attributed exclusively to co-pelletization itself. Rather, the present study establishes the performance characteristics of the composite-pellet configuration and provides a basis for future direct comparison between co-pelletized and separately fed fuel systems.

Carbon dioxide (CO_2) concentrations ranged from 7.90% for RH100 to 9.54% for ST100. These values represent the flue-gas CO_2 concentrations measured under the tested combustion conditions. No life-cycle greenhouse-gas assessment or biogenic-carbon accounting was performed in the present study; therefore, the measured CO_2 concentrations were not used to infer life-cycle carbon neutrality.

Overall, the emission results indicate a clear trade-off associated with lignite incorporation. While the pure biomass formulations exhibited lower CO and negligible SO_2 emissions, the addition of 25% lignite increased both CO and SO_2 under the tested CFBB conditions. These findings indicate that blend composition should be considered together with combustion-air and fuel-feeding control when evaluating biomass–lignite co-firing performance.

Thermogravimetric degradation behavior (DTG)

The differential thermogravimetric (DTG) analysis of the four pellet formulations, illustrated in Figure 5, reveals the thermal degradation behavior of each sample under a controlled heating rate of 10°C/min. All formulations exhibited the typical three-stage decomposition pattern associated with lignocellulosic biomass, yet with distinct variations in peak intensity and thermal transition ranges depending on blend composition.

Stage I (Below 200°C): this initial stage is attributed to the evaporation of free and bound moisture as well as the release of light volatiles. All samples exhibited minor and consistent weight loss, confirming their low moisture content and pre-conditioning prior to testing.

Stage II (200–400°C): the primary devolatilization zone corresponds to the thermal degradation of hemicellulose and cellulose. Among the samples, ST100 exhibited its main devolatilization peak at approximately 310–320 °C, whereas the corresponding peak for RH100 occurred at a slightly higher temperature.

The addition of 25% lignite to both biomass types (RH75+CP25 and ST75+CP25) resulted in delayed decomposition onset and flattened DTG peaks, reflecting the influence of lignite's more stable carbon structure and lower volatile matter. This thermal behavior is consistent with the literature noting that lignite slows down the devolatilization process in biomass–coal mixtures (Basu, 2010; Unchaisri *et al.*, 2019). Furthermore, the broadened decomposition peaks in the blends indicate overlapping degradation phases, confirming greater fuel heterogeneity.

Stage III (400–600°C): this final stage corresponds to the oxidation of residual lignin and fixed carbon. All samples demonstrated a sharp decline in weight loss beyond 500 °C, with blended formulations showing a longer tail in their DTG curves. The blended formulations exhibited extended high-temperature conversion behavior, which can be associated with the contribution of the lignite char oxidation stage. However, the burnout temperatures of ST100 and ST75+CP25 were very similar (549.9 and 550.8°C, respectively), whereas a more pronounced increase was observed for RH100 and RH75+CP25 (520.2 to 538.1°C).

The combustion indices—Ignition Index (Di), Flammability Index (C), and Comprehensive Combustion Index (S)—calculated from DTG data (Table 3) reinforce these findings. ST100 registered the highest Di (0.044), S (1.57 x 10^{-15}), and C (3.68 x 10^{-10}) values, indicating the highest overall combustion reactivity among the tested formulations. RH100 also exhibited relatively high combustion indices, with S and C values of 1.39 x 10^{-15} and 3.16 x 10^{-10}, respectively. In contrast, RH75+CP25 exhibited the lowest flammability index (2.37 × 10^{-10}), indicating lower initial combustion reactivity after lignite addition. This trend is directionally consistent with Qin *et al.* (2022), who reported improved ignition and overall combustion characteristics with increasing rice-straw fraction in bituminous coal–rice straw blends.

The thermogravimetric results showed that the effect of lignite addition was more pronounced for the RH-based formulation. The ignition temperature increased from 221 to 245°C and the burnout temperature from 520.2 to 538.1°C for RH100 and RH75+CP25, respectively. In contrast, only minor changes were observed for the ST-based formulations, with ignition and burnout temperatures increasing from 216 to 220°C and from 549.9 to 550.8°C, respectively. Together with the lower combustion indices of the lignite-containing blends, these results indicate reduced thermal reactivity after lignite incorporation, particularly for the RH-based pellets. Similar behavior has been reported for biomass–coal systems, where increasing the biomass fraction generally lowers ignition and burnout temperatures and improves combustion reactivity (Kumar and Nandi, 2022; Aich and Nandi, 2025). Guo *et al.* (2020) further showed that biomass pellet–lignite combustion involves an initial volatile-combustion stage followed by char combustion of both biomass and lignite, supporting the greater contribution of slower solid-phase oxidation as the lignite fraction increases.

Overall, the DTG analysis indicates that lignite blending moderate initial ignition and reduces combustion reactivity, while extending the high-temperature conversion stage, particularly in the RH-based blend. In contrast, pure RH and ST pellets exhibit more favorable ignition and combustion reactivity characteristics.

Conclusions

This study investigated the mechanical, thermal, and emission characteristics of rice husk (RH), rice straw (ST), and their 75% biomass + 25% lignite (CP) pellet blends in a 350 kW_{th} circulating fluidized bed boiler. RH and ST exhibited similar higher heating values of 14.84 and 14.75 MJ/kg, respectively, confirming their potential as solid biofuels. The mechanical results revealed distinct advantages for the two biomass types rather than an overall superiority of either material. RH100 exhibited a higher vertical compressive strength than ST100 (21.55 vs. 13.00 MPa), whereas ST100 showed higher abrasive resistance (98.02 vs. 94.55%). The addition of 25% lignite reduced compressive strength by approximately 4.3% for RH and 5.8% for ST and decreased abrasive resistance by 5.45 and 4.80 percentage points, respectively. Impact resistance remained high for all formulations (99.79–99.98%).

Thermogravimetric analysis demonstrated higher combustion reactivity for the pure biomass pellets than for the corresponding lignite-containing blends. RH100 and ST100 ignited at 221 and 216 °C, respectively, while 25% lignite addition increased the corresponding ignition temperatures to 245 and 220 °C. The burnout temperature increased from 520.2 to 538.1 °C for the RH-based formulation, whereas only a minor change from 549.9 to 550.8 °C was observed

for the ST-based formulation. ST100 exhibited the highest overall combustion indices, with Di = 0.044, S = 1.57×10^{-15}, and C = 3.68×10^{-10}. Overall, lignite incorporation reduced combustion reactivity and extended the high-temperature conversion stage, with a more pronounced effect on the RH-based pellets.

The CFBB emission measurements revealed a clear trade-off associated with lignite addition. CO concentrations increased from 1083.55 to 1803.96 mg/Nm³ for the RH-based fuels and from 1488.17 to 2832.42 mg/Nm³ for the ST-based fuels. SO_2 was not detected for the pure biomass pellets but reached 29.21 mg/Nm³ for RH75+CP25 and 64.30 mg/Nm³ for ST75+CP25, consistent with the sulfur introduced by lignite. NO emissions remained within a relatively narrow range of 8.01–13.77 mg/Nm³. The relatively high temporal variability of CO under the tested conditions further indicates the importance of fuel-feeding and combustion-air control for CFBB operation.

Overall, the results demonstrate a distinct trade-off associated with 25% lignite incorporation into RH- and ST-based pellets. While pellet mechanical integrity was largely retained, lignite addition reduced combustion reactivity and increased CO and SO_2 emissions under the tested CFBB conditions. The magnitude of these effects also depended on the biomass type, with the RH- and ST-based blends exhibiting different responses in ignition, burnout, and combustion indices. These findings provide quantitative evidence for evaluating biomass–lignite co-firing strategies and indicate that blend composition and combustion control should be considered jointly rather than independently. Among the formulations investigated, the pure biomass pellets provided the most favorable overall balance of mechanical integrity, combustion reactivity, and gaseous emissions. Future studies should focus on long-term combustion performance, automated air-to-fuel ratio control, optimization of fuel feeding, and detailed ash characterization under continuous operating conditions.

References

Aich S, Nandi BK, 2025. Identification of combustion characteristics of high ash Indian coal, rice straw, rice straw char and their blends. Process Saf Environ Protect 193:1243-60.

Baetge S, Kaltschmitt M, 2018. Rice straw and rice husks as energy sources - comparison of direct combustion and biogas production. Biomass Convers Bior 8:719-37.

Basu P, 2010. Biomass gasification and pyrolysis: Practical design and theory. Cambridge, Academic Press.

Beidaghy Dizaji H, Zeng T, Hartmann I, Enke D, Schliermann T, Lenz V, et al., 2019. Generation of high quality biogenic silica by combustion of rice husk and rice straw combined with pre- and post-treatment strategies - A review. Appl Sci 9:1083.

Bennamoun L, Harun NY, Afzal MT, 2018. Effect of storage conditions on moisture sorption of mixed biomass pellets. Arab J Sci Eng 43:1195-203.

Dao CN, Salam PA, Kim Oanh NT, Tabil LG, 2022. Effects of length-to-diameter ratio, pinewood sawdust, and sodium lignosulfonate on quality of rice straw pellets produced via a flat die pellet mill. Renew Energy 181:1140-54.
Do TX, Tran KT, Vu AT, Van TDS, Le ST, Nguyen QT, 2025. Effects of pelletizing conditions and additives on properties of rice straw fuel pellets and ash characteristics. Biomass Convers Bior 15:16971-85.
FAO, 2023. FAOSTAT statistical database: Crops and livestock products. Available from: https://www.fao.org/faostat/en/#data/QC
Frodeson S, Henriksson G, Berghel J, 2019. Compression of biomass substances: A study on springback effects and color formation in pellet manufacture. Appl Sci 9:4302.
Gadde B, Bonnet S, Menke C, Garivait S, 2009. Air pollutant emissions from rice straw open field burning in India, Thailand and the Philippines. Environ Pollut 157:1554-8.
Gil MV, Oulego P, Casal MD, Pevida C, Pis JJ, Rubiera F, 2010. Mechanical durability and combustion characteristics of pellets from biomass blends. Bioresour Technol 101:8859-67.
Guo F, He Y, Hassanpour A, Gardy J, Zhong Z, 2020. Thermogravimetric analysis on the co-combustion of biomass pellets with lignite and bituminous coal. Energy 197:117147.
Jadwisieńczak K, Obidziński S, Choszcz D, 2023. Assessment of the physical and energetic properties of fuel pellets made from sage waste biomass with the addition of rye bran. Materials 16:58.
Jaimes Rueda S, Rego de Vasconcelos B, Duret X, Lavoie JM, 2022. Lignin pellets for advanced thermochemical process - From a single pellet system to a laboratory-scale pellet mill. Energies 15:3007.
Jenkins BM, Baxter LL, Miles Jr TR, Miles TR, 1998. Combustion properties of biomass. Fuel Process Technol 54:17-46.
Kaniapan S, Pasupuleti J, Patma Nesan K, Abubackar HN, Umar HA, Oladosu TL, et al., 2022. A review of the sustainable utilization of rice residues for bioenergy conversion using different valorization techniques, their challenges, and techno-economic assessment. Int J Environ Res Public Health 19:3427.
Kim SJ, Park SJ, Jo SH, Yoon SJ, Moon JH, Ra HW, et al., 2024. Low-NOx emission and amorphous siliceous ash production from rice husk combustion in circulating fluidized bed system. Fuel 374:132441.
Kumar P, Nandi BK, 2022. Effect of rice husk blending on combustion characteristics of high ash Indian coal analyzed in TGA. Int J Coal Prep Util 42:3698-711.
Lim JS, Manan ZA, Alwi SRW, Hashim H, 2012. A review on utilization of biomass from rice industry as a source of renewable energy. Renew Sust Energ Rev 16:3084-94.
Liu M, Han B, Bai J, Ru J, Wang X, Xing L, et al., 2025. Investigation on the synergistic effects and thermokinetic analyses during co-combustion of corn stalk and polyethylene plastic: Effect of heating rate and placement method. Fuel 385:134032.
Mansaray KG, Ghaly AE, 1997. Physical and thermochemical properties of rice husk. Energy Sources 19:989-1004.
Mortadha H, Kerrouchi HB, Al-Othman A, Tawalbeh M, 2025. A comprehensive review of biomass pellets and their role in sustainable energy: Production, properties, environment, economics, and logistics. Waste Biomass Valoriz 16:4507-39.
Ozyuguran A, Acma HH, Dahiloğlu E, 2017. Production of fuel briquettes from rice husk-lignite blends. Environ Prog Sustain Energy 36:742-8.
Qin Z, Lei M, Zhang L, 2022. Thermogravimetric analysis of the co-combustion of bituminous coal, rice straw and sewage sludge. IOP Conf Ser Earth Environ Sci 1011:012028.
Saidur R, Abdelaziz EA, Demirbas A, Hossain MS, Mekhilef S, 2011. A review on biomass as a fuel for boilers. Renew Sust Energ Rev 15:2262-89.

Singh G, Gupta MK, Chaurasiya S, Sharma VS, Pimenov DY, 2021. Rice straw burning: a review on its global prevalence and the sustainable alternatives for its effective mitigation. Environ Sci Pollut Res 28:32125-55.
Stasiak M, Molenda M, Bańda M, Horabik J, Wiącek J, Parafiniuk P, et al., 2020. Friction and shear properties of pine biomass and pellets. Materials 13:3567.
Stolarski MJ, Stachowicz P, Dudziec P, 2022. Wood pellet quality depending on dendromass species. Renew Energy 199:498-508.
Tumuluru JS, 2018. Effect of pellet die diameter on density and durability of pellets made from high moisture woody and herbaceous biomass. Carbon Resour Convers 1:44-54.
Unchaisri T, Fukuda S, 2017. Co-firing of coal and rice straw pellet in a circulating fluidized-bed reactor. Energy Procedia 138:766-71.
Unchaisri T, Fukuda S, 2022. Investigation of ash formation and deposit characteristics in CFB co-combustion of coal with various biomass fuels. J Energy Inst 105:42-52.
Unchaisri T, Fukuda S, Phongphiphat A, Saetia S, Sajjakulnukit B, 2019. Experimental study on combustion characteristics in a CFB during co-firing of coal with biomass pellets in Thailand. Int Energy J 19:101-14.
Vassilev SV, Baxter D, Andersen LK, Vassileva CG, 2010. An overview of the chemical composition of biomass. Fuel 89:913-33.
Werther J, Saenger M, Hartge EU, Ogada T, Siagi Z, 2000. Combustion of agricultural residues. Prog Energy Combust Sci 26:1-27.
Wnorowska J, Ciukaj S, Kalisz S, 2021. Thermogravimetric analysis of solid biofuels with additive under air atmosphere. Energies 14:2257.
Zhang Y, Chen C, Qu B, Ji G, Li A, 2024. In-situ torrefaction-densification approach for pelletizing of rice hull/rice stalk and the combustion behavior analysis. Process Saf Environ Protect 183:365-77.
Zulkornain MF, Rawian NAM, Neshaeimoghaddam H, Shamsuddin AH, Saad JM, Rahman AA, et al., 2022. Influence of organic binder and moisture content on the durability of rice husk and rice straw-based pellets. Int J Appl Sci Eng 19:2021235.

Standards

ASAE S269.4 DEC96. (1996). Cubes, Pellets, and Crumbles—Definitions and Methods for Determining Density, Durability, and Moisture Content. American Society of Agricultural Engineers.
ASTM D4442-20. (2020). Standard Test Methods for Direct Moisture Content Measurement of Wood and Wood-Based Materials. ASTM International.
ASTM D3173. Standard Test Method for Moisture in the Analysis Sample of Coal and Coke. ASTM International.
ASTM D3174. Standard Test Method for Ash in the Analysis Sample of Coal and Coke from Coal. ASTM International.
ASTM D3175. Standard Test Method for Volatile Matter in the Analysis Sample of Coal and Coke. ASTM International.
ASTM D5373. Standard Test Methods for Determination of Carbon, Hydrogen and Nitrogen in Analysis Samples of Coal and Carbon in Analysis Samples of Coal and Coke. ASTM International.

ASTM D5865/D5865M-19. (2019). Standard Test Method for Gross Calorific Value of Coal and Coke. ASTM International.

ISO 17225-6:2021. (2021). Solid biofuels—Fuel specifications and classes—Part 6: Graded non-woody pellets. International Organization for Standardization.

ENplus®. ST 1001. ENplus® Wood Pellets—Requirements for Companies. European Pellet Council. (Only retained as a wood-pellet benchmark for the A1, A2, and B ash limits.)

EN 14181:2014. (2014). Stationary source emissions—Quality assurance of automated measuring systems. European Committee for Standardization (CEN).

European Parliament and Council of the European Union. (2010). Directive 2010/75/EU of the European Parliament and of the Council of 24 November 2010 on industrial emissions.

Table 1. Ultimate and proximate analyses and higher heating values of two feedstocks in blends.

Proximate analysis (%) (as received)	Rice husk (RH)	Straw (ST)	Lignite (CP)
Moisture	3.21	3.82	14.33
Volatile Matter	65.37	65.73	31.4
Fixed Carbon	15.42	14.95	17.9
Ash content	16.00	15.50	36.37
Ultimate analysis (%) (dry based)			
C	41.80	41.50	66.76
H	5.70	5.50	5.79
N	2.70	2.30	1.87
S	0.00	0.00	4.42
O (calculated by difference)	49.80	50.70	21.16
Other analysis			
HHV (MJ/kg)	14.84	14.75	13.38

Table 2. Particle diameter, length, abrasive resistance, impact resistance, and vertical compressive strength of the pellets

Pellets	Diameter (mm)	Length (mm)	Weight (g)	Abrasive resistance (%)	Impact resistance (%)	Vertical compressive strength of the pellets (MPa)
RH100	8.17±0.1	35.68±7.75	2.28±0.54	94.55	99.98	21.55±1.75
RH75+CP25	8.5±0.29	29.1±8.97	1.84±0.63	89.10	99.98	20.62±1.73
ST100	8.25±0.3	39.67±6.97	2.67±0.46	98.02	99.79	13±0.85
ST75+CP25	8.16±0.17	34.68±6.98	2.15±0.52	93.22	99.98	12.24±0.9

Table 3. The characteristic combustion parameters for four pellet blends.

Pellets	Ignition temp (°C)	Peak Temperatures (°C)			Burnout temp (°C)	DTG peak value (%/min)			Weight loss (%)			Di	S	C	
		1st	2nd	3rd		1st	2nd	3rd	1st	2nd	3rd				
RH100	221	73.13	326.9	453.2	520.2	3.54E-06	1.54E-05	8.24E-06	6.44	49.85	26.62	0.036	1.39E-1	3.16E-1	
RH75+CP25	245	70.22	329.1	464.2	538.1	3.36E-06	1.42E-05	7.14E-06	7.40	47.69	25.07	0.031	9.84E-1	2.37E-1	
ST100	216	68.56	318.8	419.8	549.9	3.67E-06	1.71E-05	6.77E-06	5.46	52.90	21.92	0.044	1.57E-1	3.68E-1	
ST75+CP25	220	75.72	309.8	451.4	550.8	3.99E-06	1.6 E-05	5.05E-06	7.41	51.55	22.47	0.040	1.34E-1	3.31E-1	

Table 4. Emissions from the combustion of fuel mixtures in CFBB.

Pellets	CO_2 (%)	SO_2 (mg/Nm^3)	CO (mg/Nm^3)	NO (mg/Nm^3)
RH100	7.90±2.60	-	1083.55±1252	8.79±2.20
RH75+CP25	8.28±2.82	29.21±4.87	1803.96±2477	13.77±3.70
ST100	9.54±2.85	-	1488.17±1211	8.01±2.05
ST75+CP25	8.51±2.88	64.3±32.60	2832.42±5447	9.22±2.93

Values are reported as mean ± SD of pooled 1-s measurements obtained during three 30-min measurement periods.



Figure 1. Representative photographs of the pellet formulations investigated in this study. **a)** RH100; **b)** RH75+CP25; **c)** ST100; **d)** ST75+CP25.



Figure 2. Actual photograph of the commercial-scale flat-die pelletization system used for production of the RH-, ST-, and lignite-containing pellet formulations.



Figure 3. Actual photograph of the pilot-scale 350 kW_{th} circulating fluidized bed boiler (CFBB) experimental system used for combustion testing of the pellet formulations.

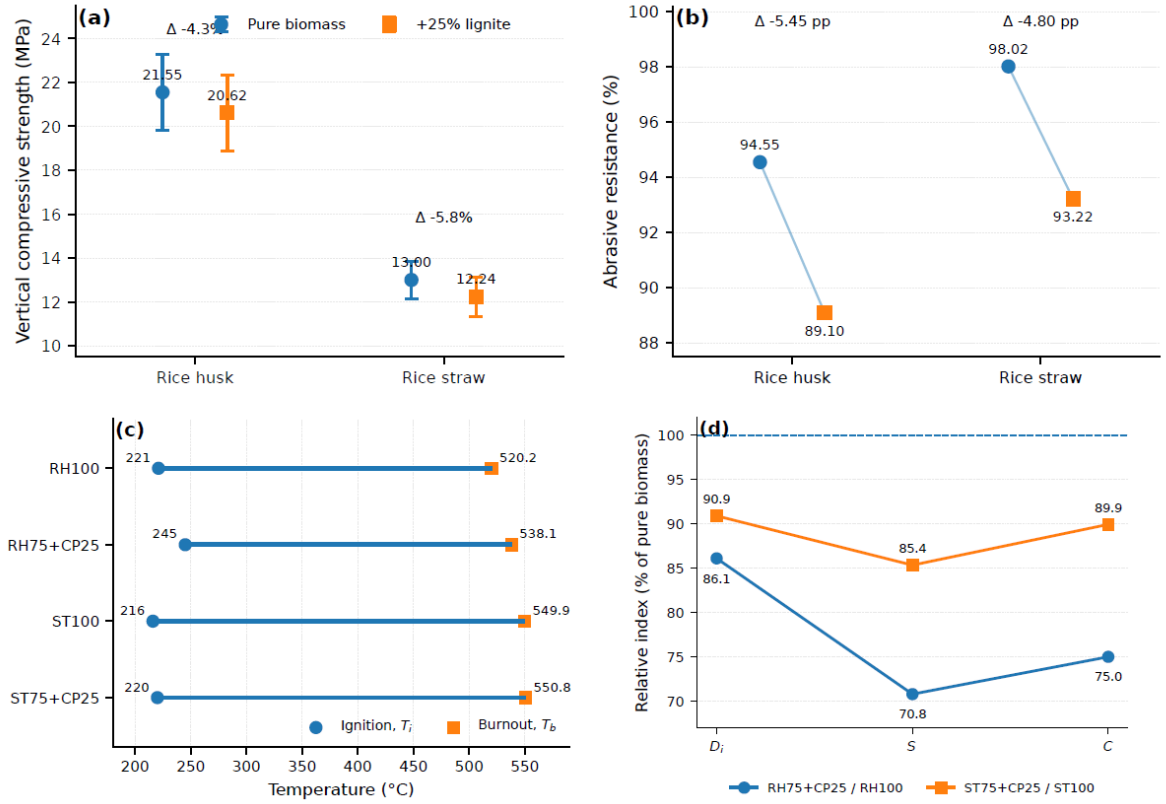


Figure 4. Mechanical and combustion performance of RH- and ST-based pellets with and without 25% lignite addition. **a)** Vertical compressive strength. **b)** Abrasive resistance. **c)** Ignition and burnout temperatures. **(d)** Relative combustion indices.

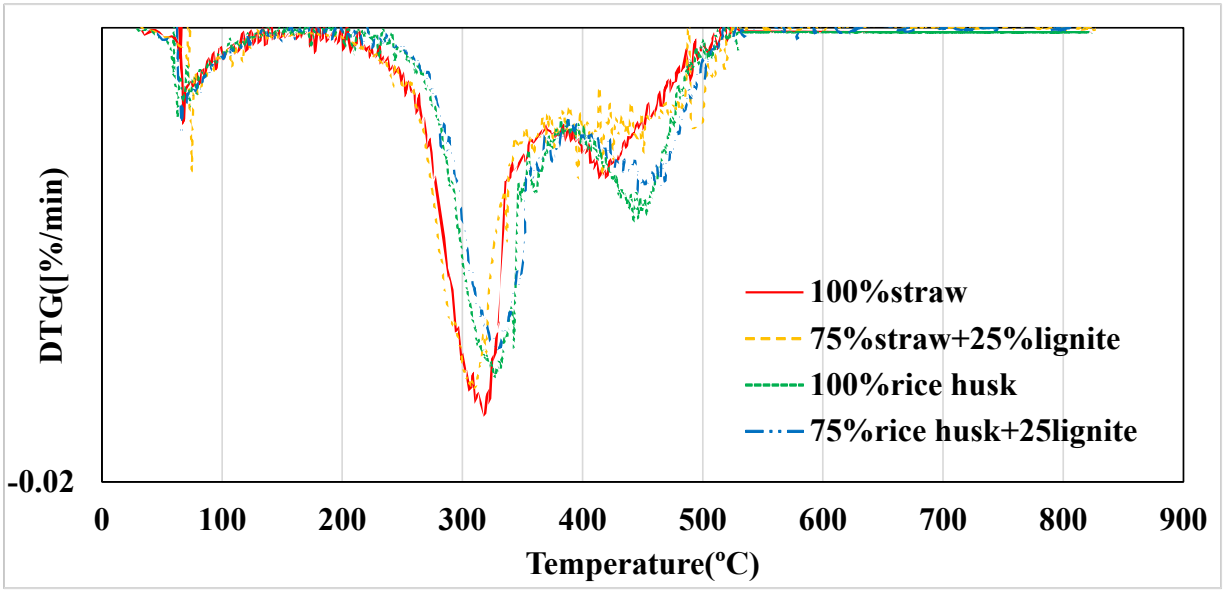


Figure 5. DTG curves of fuel mixtures at 10ºC/min heating rate.